Broadband dielectric spectroscopy on glycerol and CKN

Andrei Pimenov, Peter Lunkenheimer, Alois Loidl

Angaben zur Veröffentlichung / Publication details:

Pimenov, Andrei, Peter Lunkenheimer, and Alois Loidl. 1996. "Broadband dielectric spectroscopy on glycerol and CKN." *Ferroelectrics* 176 (1): 33–41. https://doi.org/10.1080/00150199608223598.

BROADBAND DIELECTRIC SPECTROSCOPY ON GLYCEROL AND CKN

A. PIMENOV, P. LUNKENHEIMER and A. LOIDL
Institut für Festkörperphysik, Technische Hochschule Darmstadt, D-64289 Darmstadt, Germany

The dielectric susceptibility of supercooled glycerol and of the glassy ionic conductor $[Ca(NO_3)_2]_{0.4}$-$[KNO_3]_{0.6}$ has been measured for frequencies 3 μHz < ν < 40 GHz and temperatures 100 K < T < 500 K. In glycerol the dielectric susceptibility differs significantly from that obtained from neutron and light-scattering techniques. Hence, we conclude, that in glycerol the dipolar relaxations are only weakly coupled to density fluctuations. In contrast, the conductivity relaxation in CKN yields a susceptibility which compares well with neutron and light-scattering techniques and thus seems to be fully coupled to the structural relaxation. The dielectric results in CKN can be described using the scaling predictions of the mode-coupling theory.

At present, the relaxation dynamics of glass forming liquids is a matter of stimulating controversy.[1] On the experimental side, it is still to be proven, if the response functions measured by different techniques can be directly compared. In parallel to the experimental progress, microscopic theories, phenomenological models and scaling theories were developed making distinct predictions concerning the relaxation dynamics at the glass transition.[1]

During the last decade the mode-coupling theory (MCT)[2] has been established which describes the liquid to glass transition as a dynamic phase transition. The MCT is based on a self-consistent treatment of nonlinear interactions between fluctuations and reveals a transition into a nonergodic glass state at a critical temperature T_c which is well above the calorimetric glass transition temperature T_g. T_c is characterized by a bifurcation point at which the dynamics separates into a slow (α-relaxation) and a fast component (microscopic peak). MCT makes very precise predictions concerning the shape and the temperature dependence of the dynamical susceptibility. To verify or disprove MCT should be a challenge to every experimentalist working in the field of the glass transition.

Neutron scattering results seem to be in accord with the predictions of MCT.[3] The most convincing experimental evidence of critical dynamics close to the glass transition has been provided by light-scattering experiments by Cummins and coworkers.[4] Contrary, dielectric experiments did not reveal clear experimental evidence for critical dynamics in viscous liquids above T_g.[5] Of course, this is due to the fact, that dielectric spectroscopy, although covering sometimes 15 decades in frequency, usually does not extend to the high frequency range (10 GHz) where the scaling predictions can be tested.

Glycerol $[C_3H_5(OH)_3]$, with a melting temperature T_m = 291 K and a calorimetric phase transition at $T_g \approx$ 185 K is a hydrogen-bonded material, that easily can be supercooled and has been investigated in numerous attempts to verify models and theories of phase transition. Glycerol has been used by Kremer, Schönhals and oth-

ers[5,6] to show, that the dielectric results are not in accordance with the predictions of MCT and by Wuttke *et al.*[7] and Rössler *et al.*[8] to evidence, that light scattering data do qualitatively resemble the mode-coupling scenario. Binary mixtures of potassium nitrate KNO_3 and calcium nitrate $Ca(NO_3)_2$ are well studied ionic conducting samples.[9] Specifically, the ionic mixture $[Ca(NO_3)_2]_{0.4}(KNO_3)_{0.6}$, abbreviated as CKN, is easily to vitrify and was one of the first glass formers on which MCT has been successfully tested using neutron[10] and light scattering techniques.[4] From these results the critical temperature T_c = 375 K has been determined. The calorimetric glass transition temperature is close to 330 K. For comparison with theory it seems important to investigate systems characterized by dipolar reorientation as well as systems where ionic diffusion dominates.

We investigated the complex dielectric permittivity $\varepsilon^* = \varepsilon' + i\varepsilon''$ of glycerol and CKN for frequencies $3 \cdot 10^{-6}$ Hz $\leq \nu \leq 4 \cdot 10^{10}$ Hz. The aim was to directly compare the dielectric loss, $\varepsilon''(\nu, T)$ with the imaginary part of the dynamic susceptibility, $\tilde{\chi}''(\nu, T)$, as observed by neutron and light-scattering techniques.

The measurements have been performed using the time domain technique ($3 \cdot 10^{-6}$–100 Hz), commercially available LCR meters (10^{-2} Hz–10 MHz), network analyzers (1 MHz–10 GHz) and standard microwave techniques (6–40 GHz). To cover the complete frequency range, a single $\varepsilon''(\nu)$ curve at a given temperature is superimposed using results from different experimental setups. Due to the different geometrical capacities it was necessary to shift the ε'' values of the different measurements with respect to each other to construct a $\varepsilon''(\nu)$ curve. This is crucial if no overlap exists between the data sets and it is important to note, that we shifted the complete data sets, $\varepsilon''(\nu, T)$, by one constant factor only.

A further problem arises when the dielectric data of ionically conducting CKN samples are presented. In ionic conductors the strong dc-conductivity makes the observation of α-relaxation processes almost impossible. In addition, the low-frequency data are strongly influenced by spurious effects, e.g. blocking electrodes. To avoid these problems, the dielectric data are usually presented in terms of the complex electrical modulus $M^* = 1/\varepsilon^*$. M^* represents the conductivity relaxation[11] and when the dc conductivity is strongly coupled to the structural relaxation, the peak in M'' closely follows the α-relaxation. However, one has to mention, that there exists an unsettled controversy concerning the "ideal" dielectric behavior of ionic conductors and the use of the electrical modulus formalism.[12,13] For high frequencies, $\varepsilon' \approx \varepsilon_\infty$, $\varepsilon'' < \varepsilon'$ and $M^* \approx \varepsilon''(\nu)/\varepsilon_\infty^2$ and hence, the frequency dependence of M'' results mainly from $\varepsilon''(\nu)$, thus making both representations equivalent in that frequency region.

Figures 1 and 2 show the measured frequency dependence of the imaginary part of the dielectric constant ε'' for glycerol and of the dielectric modulus M'' for CKN in a double-logarithmic plot. The data reveal the dramatic slowing down of the relaxation processes, namely the α-relaxation in glycerol and the conductivity relaxation in CKN. The regime close to the relaxation maximum can be described by the Fourier transform of the Kohlrausch-Williams-Watts (KWW) function $\phi_0 \exp(-t/\tau)^\beta$, with the stretching exponent β and the mean relaxation time τ. The temperature dependence of τ can roughly be described using a Vogel-Fulcher equation $\tau = \tau_0 \cdot \exp[E_B/(T - T_{VF})]$ with Vogel-Fulcher temperatures T_{VF} = 131 K and 286 K for glycerol and CKN, respectively. The high-frequency wing of the relaxation process

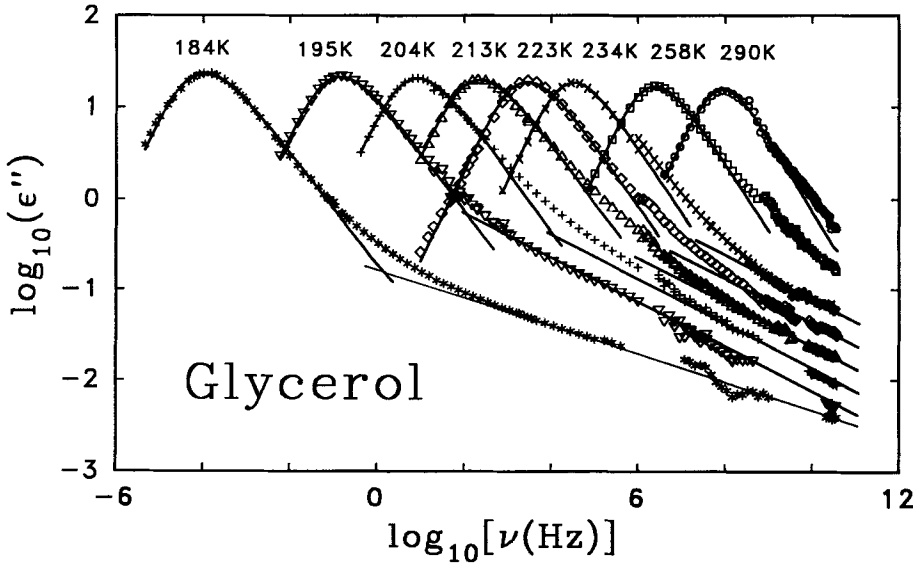

FIGURE 1 Frequency dependence of the dielectric loss in glycerol in a double logarithmic representation. The solid lines represent a KWW-fit for the peak maxima and a power-law behavior of the dielectric loss at the high-frequency tail.

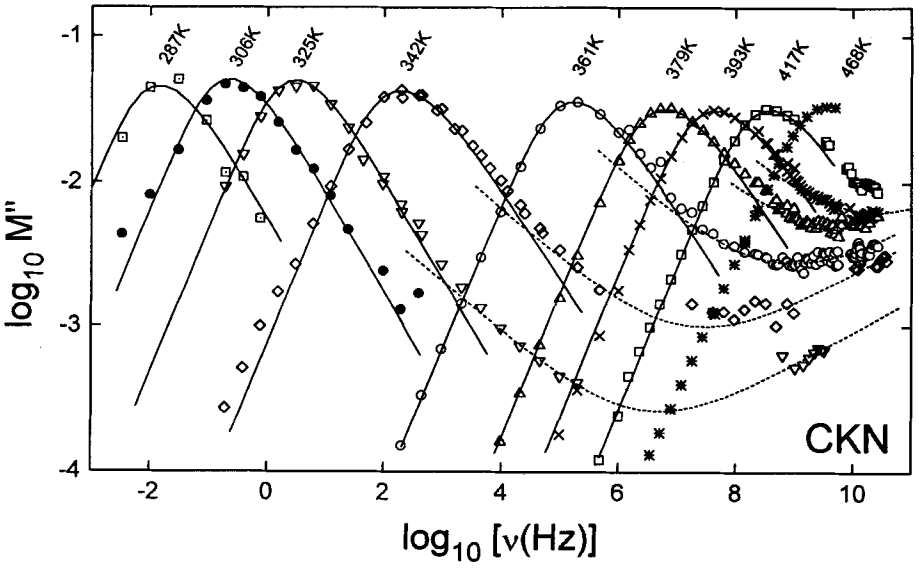

FIGURE 2 Frequency dependence of the imaginary part of the electrical modulus M'' in CKN in a double-logarithmic plot. The solid lines represent KWW fits. The dashed lines have been calculated according to the interpolation formula for the β-minimum (Equation (1), $a = 0.23$, $b = 0.35$). The lines below $T_c (T_c \sim 360$ K) are only plotted for presentation purposes, i.e. to guide the eye.

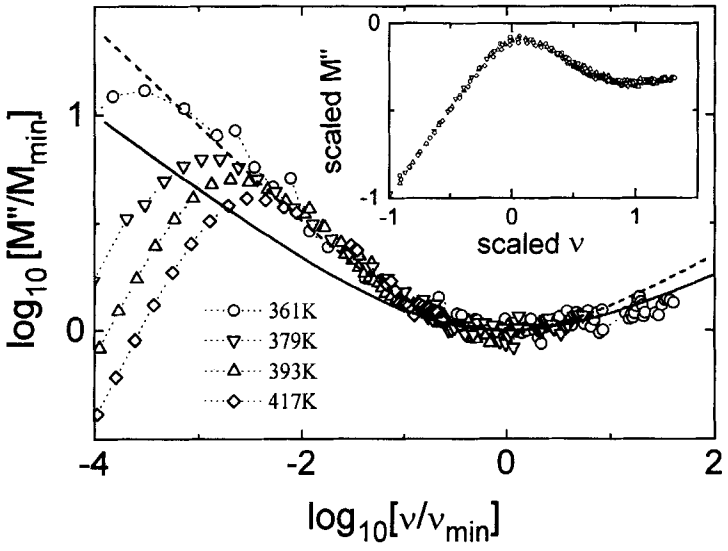

FIGURE 3 Master plot of the data for M'' of CKN at temperatures from 361 to 417 K. The solid line represents the result of a fit according to predictions of the MCT, Equation (1). The resulting parameters a and b are 0.23 and 0.35, respectively. The dashed line indicates a best fit to the light scattering data (Reference 4, $a = 0.273$, $b = 0.458$). The insert shows the result of the scaling procedure as described in the text, allowing to superimpose both minima and maxima of M'' simultaneously.

reveals significant deviations from a KWW type of behavior (solid line through the peak maxima) and indications of a second power law with an exponent $b \approx 0.25$ in glycerol and a minimum at the highest frequencies in CKN. In CKN the minimum is well established for the temperatures between 342 K and 393 K, and is very similar to that observed with neutron[10] and light scattering techniques.[4]

Although we measured a limited set of temperature scans only, we tried to compare the CKN results with the scaling predictions of the MCT. First of all we fitted the minima in the $\varepsilon''(\omega)$ representation using the interpolation formula for the so called β-minimum, which interpolates the imaginary part of the dynamic susceptibility between two asymptotic power laws with exponents $(-b)$ and a:

$$\varepsilon''(\nu) = \varepsilon''_{\min}[a(\nu/\nu_{\min})^{-b} + b(\nu/\nu_{\min})^{a}]/(a + b) \tag{1}$$

We fitted the ε'' curves close to the minimum using Equation (1) and found a consistent description using $a = 0.23$, $b = 0.35$. Within the experimental uncertainties $\varepsilon''_{\min} \propto (T - T_c)^{0.5}$, and $\nu_{\min} \propto (T - T_c)^{1/2a}$ with $T_c \approx 360$ K, which are further predictions of MCT. The parameters a and b are related via the Gamma functions and reveal a unique exponent parameter, the system parameter of CKN, $\lambda = 0.87$:

$$\lambda = \Gamma^2(1 - a)/\Gamma(1 - 2a) = \Gamma^2(1 + b)/\Gamma(1 + 2b) \tag{2}$$

That the scaling relation can be applied is documented in Figure 3, where we constructed a master curve. The solid line indicates the result of a fit using the interpolation formula Equation (1). The dashed line is the result of the best fit of Equation (1) to the light scattering results of Cummins and coworkers.[4] They found in their analysis $a = 0.273$, $b = 0.458$, $\lambda = 0.811$ and $T_c = 378$ K. The calculated frequency dependence of the dielectric susceptibility using Equation (1) is also pre-

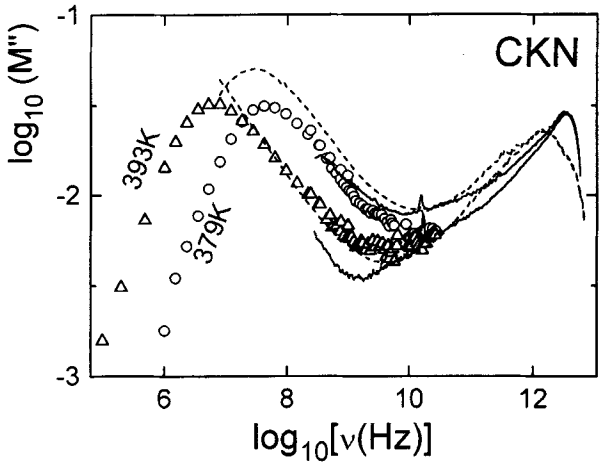

FIGURE 4 Comparison of the dielectric results (M'') with the susceptibiltiy $\tilde{\chi}''$ obtained from neutron scattering (dashed lines)[10] and from light scattering (solid lines).[4] The dielectric data were measured at 379 K and 393 K. Light scattering and neutron scattering data were taken at 383 K and at 403 K, respectively.

sented as dashed lines in Figure 1. However, these lines should be taken merely as a guide to the eye because i) at lower frequencies $M''(\nu)$ and $\varepsilon''(\nu)$ will deviate significantly and ii) for $T < T_c$ the scaling relation as given by Equation (1) cannot be used.

It is known, that the dielectric data of glycerol can be scaled onto a single master curve using the scaling as proposed by Nagel and coworkers.[14] The modulus data of CKN for $T > T_c$ have the same slope for $\nu < \nu_{max}$, $\nu_{max} < \nu < \nu_{min}$ and $\nu > \nu_{min}$ respectively. In this case it is possible to scale the spectra on a single curve with a transformation of the type: $\mathbf{r}_1 = (\mathbf{r}_0 + \mathbf{s})\cdot k$, where $\mathbf{s}$ and k are transformation vector and factor respectively. To scale the CKN data we have used the coordinates:

$$\log(\nu_{min}/\nu_{max})\cdot[\log(M''/2M_{max})] \text{ vs } \log(\nu_{min}/\nu_{max})\cdot[\log(\nu/\nu_{max})] \qquad (3)$$

The result of this scaling procedure is shown in the insert of Figure 3.

Figure 4 shows log M'' vs log ν for CKN, compared to dynamical susceptibilities, determined from neutron (dashed lines, Reference 10) and light scattering experiments (solid lines, Reference 4) for two temperature. Despite some smaller deviations, all three data sets reveal a striking similarity. Not only the minima coincide, but also the relaxation maxima are observed at similar frequences. This again demonstrates that conductivity relaxation and structural relaxation are strongly coupled in CKN. Figure 4 reveals unambiguously that the relevant frequency range to test the MCT predictions can be covered by dielectric measurements.

The temperature dependence of the fitting parameters of the KWW function to the M'' spectra of CKN and the T-dependence of the dc conductivity are shown in Figures 5 and 6. Within the MCT, the critical behavior should also be observed in the temperature dependence of the maximum of the dielectric loss. For $T > T_c$, the theory predicts $\tau^{-1} \propto \nu_{max} \propto (T - T_c)^{\gamma}$, with $\gamma = 1/2a + 1/2b$. For $T < T_c$ it is expected that thermally activated processes start to dominate. Figure 5 shows the results of fits as solid lines. Indeed, for $T > T_c$ the data are consistent with the mode

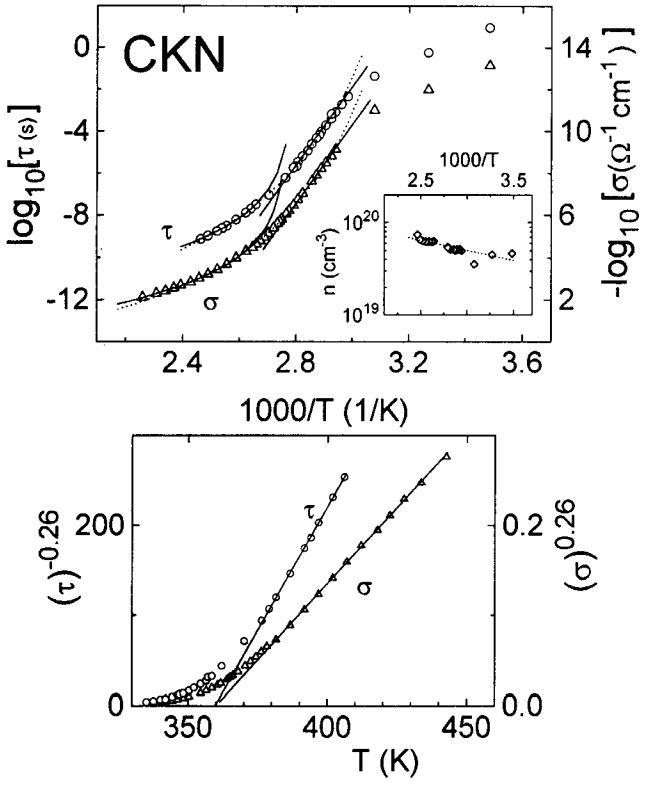

FIGURE 5 Upper frame: temperature dependence of the mean relaxation rate and the dc-conductivity of CKN in an Arrhenius-type representation. The solid lines represent critical slowing down ($T > T_c$) and thermally activated behavior ($T < T_c$). The dashed line represents a fit using a Vogel-Fulcher law with an energy barrier $E \approx 1350$ K and a Vogel-Fulcher temperature $T_{VF} = 287$ K. The inset demonstrates the effective density of mobile ions, calculated from Einstein relation within the simplest approximation: $\sigma_{dc} \approx (ne^2d^2/kT)(1/\tau)$, where $d \approx 4.6$ Å is the effective size of NO_3 complex.[15] Lower frame: the scaling behavior of τ and σ_{dc} for temperatures above T_c. The data reveal a linear increase when plotted as $\tau^{-1/\gamma}$ and $\sigma^{1/\gamma}$ vs T, with $\gamma = 3.6$.

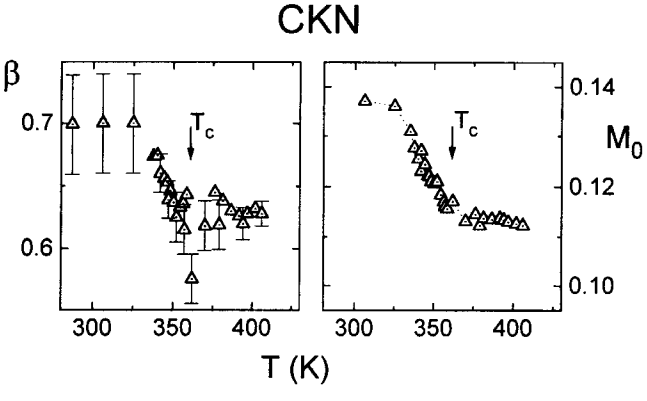

FIGURE 6 Temperature dependence of the KWW-fit parameters for CKN: stretching exponent β and $M_0 = 1/\varepsilon_\infty$. The arrows indicate the MCT transition temperature $T_c \approx 360$ K.

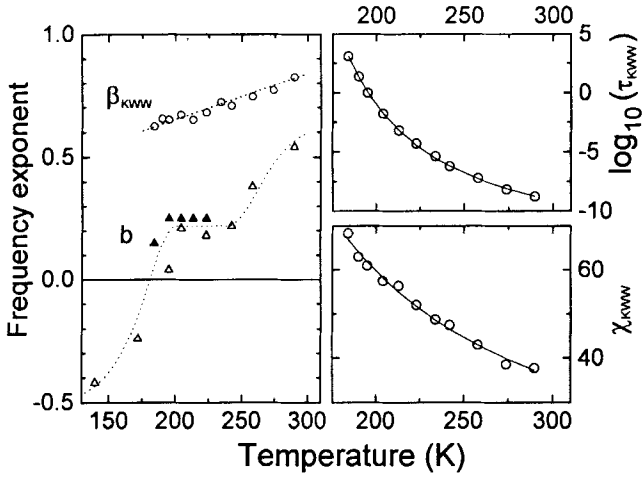

FIGURE 7 Temperature dependence of the KWW-fit parameters for glycerol: stretching exponent β_{KWW}, relaxation rate τ_{KWW} and "static" susceptibiltiy χ_{KWW}. The high frequency power law exponents b are taken from data of Figure 1 (closed triangles) and Figure 8 (open triangles).

coupling expression. For $T < T_c$ thermally activated behavior is observed. In the lower part of Figure 5 we plotted $\tau^{-1/\gamma}$ and $\sigma^{1/\gamma}$ vs T and again find a linear dependence for $T > T_c$. On the basis of these results, also the interpretation of the temperature dependence of β (Figure 6) can be given: β is constant for $T > T_c$, increases below T_c possibly due to thermally activated hopping and tails off at a constant value below the thermodynamic glass transition when the conductivity relaxation is decoupled from the structural relaxation.

The results of the KWW fits for the glycerol data (Figure 1), namely the stretching exponent β_{KWW}, the mean relaxation time τ_{KWW} and the "static" susceptibility χ_{KWW} (the area under the KWW peak) are presented at Figure 7. In the temperature region investigated and with decreasing temperature, β_{KWW} decreases from 0.8 to approximately 0.55 at T_g, while τ_{KWW} follows a Vogel-Fulcher law with a Vogel-Fulcher temperature T_{VF} = 131 K. β_{KWW} and τ_{KWW} are in close agreement with published data. The high frequency wing of $\varepsilon''(\nu)$ was described with a power law behavior, with an exponent b. b is significally smaller than the exponent β_{KWW} which describes the high frequency wing of the KWW function. The KWW function (transformed into the frequency domain) and the high-frequency power law are indicated as solid lines in Figure 1. The results are shown in Figure 7: b is almost constant for $T > T_g$, but changes significantly for lower temperatures. Figure 7 also shows the frequency exponent as extracted from the high frequency results (6–40 GHz, Figure 8).

The high-frequency spectra of glycerol are shown in Figure 8. The lines indicate a simple power law behavior $\varepsilon'' \approx \nu^s$. It is clear, that at room temperature the frequency dependence is strongly influenced by the α-relaxation (see Figure 1). The mean relaxation rate at 290 K is close to 100 MHz and reaches a value of 30 GHz at approximately 425 K. Between 242 and 200 K, the slope coincides with the slope as determined at lower frequencies ($b \approx 0.25$). Approximately at T_g, ε'' becomes constant and a negative slope develops for $T < T_g$, thus revealing a minimum in ε'' passing through the frequency regime investigated.

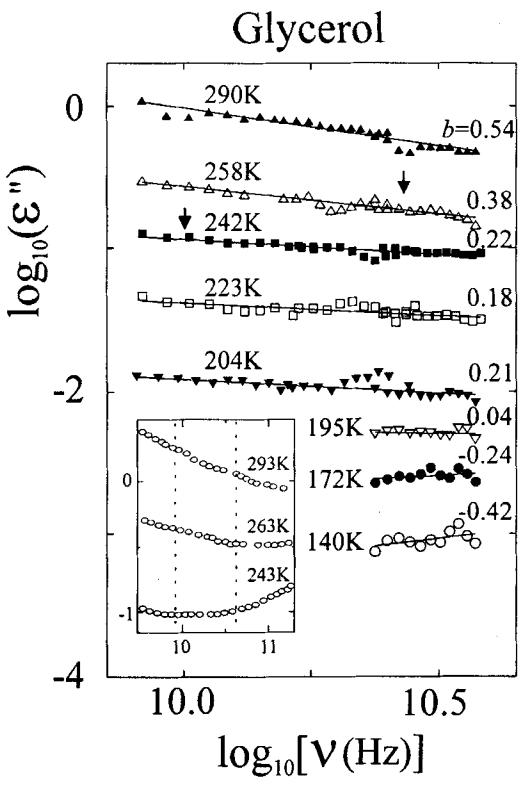

FIGURE 8 Frequency dependence of the dielectric loss in glycerol between 8 and 40 GHz on a double-lorarithmic plot. The solid lines indicate a power law behavior ν^b, taking only the high frequency data into account. The arrows at the 258 K and 242 K data indicate the frequencies at which minima in the susceptibilities have been observed by neutron and light scattering investigations. The inset shows the-light scattering results in the same frequency regime and at comparable temperatures (taken from Reference 7).

The results of Figure 8 can be compared to the results as observed from the neutron and light scattering experiments (inset in Figure 8).[7] the arrows, at the 258 and 242 data sets, indicate the minima observed with the latter techniques. The dielectric results in glycerol exhibit no minimum in $\varepsilon''(T)$ at $T > T_g$. Obviously for glycerol the dielectric loss $\varepsilon''(\nu)$ is a different quantity than the dynamical susceptibiltiy $\chi''(\nu)$ as calculated from neutron and light-scattering experiments. This is also clear by comparing the relative temperature dependence of ε'' (30 GHz) and $\tilde{\chi}''$ (30 GHz).[7] Between room temperature and T_g, ε'' decreases by three orders of magnitude, χ'' only by one. It is important to note, that i) the slope as determined dielectrically is in rough agreement with the slope b as determined from the neutron and the light scattering results and ii) b changes drastically for $T < T_g$. It approaches zero close to T_g and becomes even negative for further decreasing temperatures. A zero slope would meet the predictions of Menon and Nagel[16] concerning a divergence of the static susceptibility, which is equivalent to the nonzero nonergodicity parameter f_c of the MCT theory.

We conclude, that in contrast to the data on glycerol, the CKN results measured by dielectric spectroscopy are in close agreement with the theoretical predictions of

MCT and the susceptibility spectra, calculated in light and neutron scattering experiments. Obviously, this is due to the fact that ionic motion is directly coupled to the density fluctuations which are probed by light and neutron scattering spectroscopy and are calculated in the mode-coupling theory. This strong coupling of the dipolar relaxations to transitional degrees of freedom is absent in supercooled liquids like glycerol.

ACKNOWLEDGEMENT

This research was partly supported by the Sonderforschungsbereich 262.

REFERENCES

1. See e.g. "Relaxations in Complex Systems," Vols. 1 and 2, K. L. Ngai, E. Riande and G. B. Wright, eds., *J. Non-Cryst. Solids*, **172–174** (1994).
2. For a review see: W. Götze and L. Sjögren, *Rep. Progr. Phys.*, **55**, 241 (1992).
3. For a review see: W. Petry and J. Wuttke, *Transp. Theory Statist. Phys.*, 1995, in print.
4. G. Li, W. M. Du, X. K. Chen, H. Z. Cummins and N. Z. Tao, *Phys. Rev. A*, **54**, 3867 (1992).
5. A. Hoffmann, F. Kremer, E. W. Fischer and A. Schönhals in "Disorder Effects on Relaxational Processes," R. Richert and A. Blume eds., Springer Verlag, Berlin, 1994, p. 301.
6. A. Schönhals, F. Kremer, A. Hoffmann, E. W. Fischer and E. Schlosser, *Phys. Rev. Lett.*, **70**, 3459 (1993).
7. J. Wuttke, J. Hernandes, G. Li, G. Goddens, H. Z. Cummins, F. Fujara, W. Petry and H. Sillescu, *Phys. Rev. Lett.*, **72**, 3052 (1994).
8. E. Rössler, A. P. Sokolov, A. Kislink and D. Quitmann, *Phys. Rev. B*, **49**, 14967 (1994).
9. F. S. Nowell, R. A. Bose, P. B. Macedo and C. Moynihan, *J. Phys. Chem.*, **78**, 639 (1974).
10. F. Mezei, W. Knaak and B. Forego, *Phys. Rev. Lett.*, **58**, 571 (1987); W. Knaak in "Dynamics of Disordered Materials," D. Richter, A. J. Dianoux, W. Petry and J. Teixeira, eds., Springer Proceedings in Physics, Vol. 37, Berlin, Heidelberg, 1989, p. 64.
11. P. B. Macedo, C. T. Moynihan and R. Bose, *Phys. Chem. Glasses*, **13**, 171 (1972); C. T. Moynihan, *J. Non-Cryst. Solids*, **172–174**, 1395 (1994).
12. S. R. Eliott, *J. Non-Cryst. Solids*, **170**, 97 (1994).
13. C. A. Angell, *Chem. Rev.*, **90**, 523 (1990).
14. N. Menon, K. P. O'Brien, P. K. Dixon, L. Wu, S. R. Nagel, B. D. Williams and J. P. Carini, *J. Non-Cryst. Solids*, **141**, 61 (1992).
15. E. Rhodes, W. E. Smith and A. R. Ubbelohde, *Proc. Roy. Soc. A*, **285**, 263 (1965).
16. N. Menon and S. R. Nagel, *Phys. Rev. Lett.*, **74**, 1230 (1995).